7 June 1996

ELSEVIER

Chemical Physics Letters 255 (1996) 71–78

CHEMICAL PHYSICS LETTERS

Analytical solutions for spin 3/2 off-resonance line intensities in solid state NMR

S.Z. Ageev, B.C. Sanctuary

Department of Chemistry, McGill University, Montreal, PQ, Canada H3A 2K6

Received 15 February 1996; in final form 11 March 1996

Abstract

The density matrix of a spin 3/2 subject to a first-order quadrupole interaction in solids and excited by an off-resonance rf pulse, is calculated analytically using the algebraic computer program MAPLE. The results are valid for arbitrary values of the rf amplitude, ω_1, quadrupolar coupling, ω_Q, and offset, $\Delta\omega$, and applied to the analysis of cases where the offset term is not negligible. The treatment can be readily modified to include a second-order quadrupolar interaction during the pulse.

1. Introduction

Quadrupolar nuclei are multilevel systems with unequal spacing between the energy levels caused by the presence of the quadrupolar interaction. The density matrix of a spin 3/2 subject to the first-order quadrupolar interaction while the rf pulse is on, was calculated by Man [1]. Later he extended his calculations to two pulse sequences retaining the secular part of the heteronuclear interaction during the evolution period between the pulses [2]. His results are valid for any ratio of quadrupolar coupling to the applied rf field amplitude, ω_Q/ω_1, and can be used for the determination of quadrupolar parameters from 1D nutation experiments [1]. However, his calculations are valid for on-resonance excitation conditions only. His treatment uses the fictitious spin 1/2 operator formalism [3]. Here, based on the application of computer algebra and simple matrix methods, we calculate the response of a spin 3/2, taking into account the resonance offset and the first-order quadrupolar interaction during the pulse. Our results are valid for any ratios of ω_Q/ω_1 and $\Delta\omega/\omega_1$. The offset term is relevant for accounting for the secular part of the heteronuclear interaction and/or the static magnetic field inhomogeneity while the pulse is on [2]. Moreover, our results are readily modified to include the second-order quadrupolar interaction during the pulse. The conclusions of our studies should be useful for Raman NMR studies of a spin 3/2 [4] and for off-resonance nutation experiments performed by Kentgens [5].

2. Theory

The Hamiltonian for a system excited by an rf pulse in the rotating frame associated with the central transition, and neglecting high frequency terms, is

$$H^{(\phi)} = H_Q^{(1)} + H_{rf}^{(\phi)}, \tag{1}$$

PII S0009-2614(96)00334-X

where

$$H_Q^{(1)} = \tfrac{1}{3}\omega_Q\left[3I_z^2 - I(I+1)\right],$$

$$\omega_Q = \frac{3e^2qQ}{8I(2I-1)\hbar} \times\left(3\cos^2\beta - 1 + \eta\sin^2\beta\cos 2\alpha\right),$$

$$H_{rf}^{(\phi)} = \Delta\omega I_z - \omega_1\left(I_x\cos\phi + I_y\sin\phi\right).$$

The Euler angles α and β describe the static magnetic field with respect to the quadrupolar principal axis system (QPAS); the rf amplitude ω_1, phase ϕ and offset $\Delta\omega$ describe a pulse. Here $H_Q^{(1)}$ is the first-order quadrupolar Hamiltonian, $e^2qQ/\hbar$ is the quadrupolar coupling constant, ω_Q is the quadrupolar coupling and η is the asymmetry parameter. Angular frequency units are used and the effects of relaxation and second-order quadrupolar interaction are ignored in this Letter.

The dynamics of the spin 3/2 system under a pulse along the positive x-axis ($\phi = 0$) is given by the density matrix

$$\rho_0(t) = e^{-iH^{(0)}t/\hbar}\rho(0)e^{iH^{(0)}t/\hbar} \tag{2}$$

with the initial condition $\rho(0) = I_z$. The matrix representation of $H^{(0)}$ is given in Table 1. The four eigenvalues of $H^{(0)}$ can be obtained using the results of Ref. [6] and are found to be

$$E_1 = (R+D)/2,$$
$$E_2 = (R-D)/2,$$
$$E_3 = -(R-S)/2,$$
$$E_4 = -(R+S)/2. \tag{3}$$

The various constants are

$$D = \left[\frac{1}{2}\left(X + \frac{Y}{R}\right) - R^2\right]^{1/2},$$

$$S = \left[\frac{1}{2}\left(X - \frac{Y}{R}\right) - R^2\right]^{1/2}, \tag{4}$$

and

$$R = 6^{-1/2}\left[X + \left(X^2 + 12Z\right)^{1/2}\cos(\delta/3)\right]^{1/2}, \tag{5}$$

where

$$\cos\delta = -\left[X^3 - 36XZ - 54Y^2\right]/\left(X^2 + 12Z\right)^{3/2}. \tag{6}$$

Here X, Y and Z depend on the interaction parameters as

$$X = -4\left(-\tfrac{5}{2}\Delta\omega^2 - 2\omega_Q^2 - \tfrac{5}{2}\omega_1^2\right),$$
$$Y = -4\left(-4\Delta\omega^2\omega_Q + 2\omega_Q\omega_1^2\right),$$
$$Z = 16\left(\tfrac{9}{8}\Delta\omega^2\omega_1^2 + \omega_Q^4 - \tfrac{5}{2}\Delta\omega^2\omega_Q^2 + \tfrac{9}{16}\omega_1^4 + \tfrac{9}{16}\Delta\omega^4 + \tfrac{1}{2}\omega_Q^2\omega_1^2\right). \tag{7}$$

The energies E_1, E_2, E_3 and E_4 are ordered as $E_1 \geq E_2 \geq E_3 \geq E_4$. These eigenvalues are the generalization of the result of Ref. [3] and valid for any ratios of ω_Q/ω_1 and $\Delta\omega/\omega_1$.

The components of the normalized eigenvectors associated with these four eigenvalues are

$$X_i = 1/N_i.$$
$$Y_i = (-a/b)/N_i,$$
$$Z_i = (b - ca/b)/\omega_i N_i,$$
$$T_i = b(b - ca/b)\,gN_i, \tag{8}$$

where $i = 1, 2, 3$ and 4, the values N_i are chosen to normalize each eigenvector and

$$a = \tfrac{3}{2}\Delta\omega + \omega_Q - E_i,$$
$$b = -\sqrt{3}\,\omega_1,$$
$$c = \tfrac{1}{2}\Delta\omega - \omega_Q - E_i,$$
$$d = -\tfrac{1}{2}\Delta\omega - \omega_Q - E_i,$$
$$g = -\tfrac{3}{2}\Delta\omega + \omega_Q - E_i. \tag{9}$$

Table 1
The matrix form of the Hamiltonian $H^{(0)}$

$$H^{(0)} = \begin{pmatrix} \frac{3}{2}\Delta\omega + \omega_Q & -\frac{1}{2}\sqrt{3}\,\omega_1 & 0 & 0 \\ -\frac{1}{2}\sqrt{3}\,\omega_1 & \frac{1}{2}\Delta\omega - \omega_Q & -\omega_1 & 0 \\ 0 & -\omega_1 & -\frac{1}{2}\Delta\omega - \omega_Q & -\frac{1}{2}\sqrt{3}\,\omega_1 \\ 0 & 0 & -\frac{1}{2}\sqrt{3}\,\omega_1 & -\frac{3}{2}\Delta\omega + \omega_Q \end{pmatrix}$$

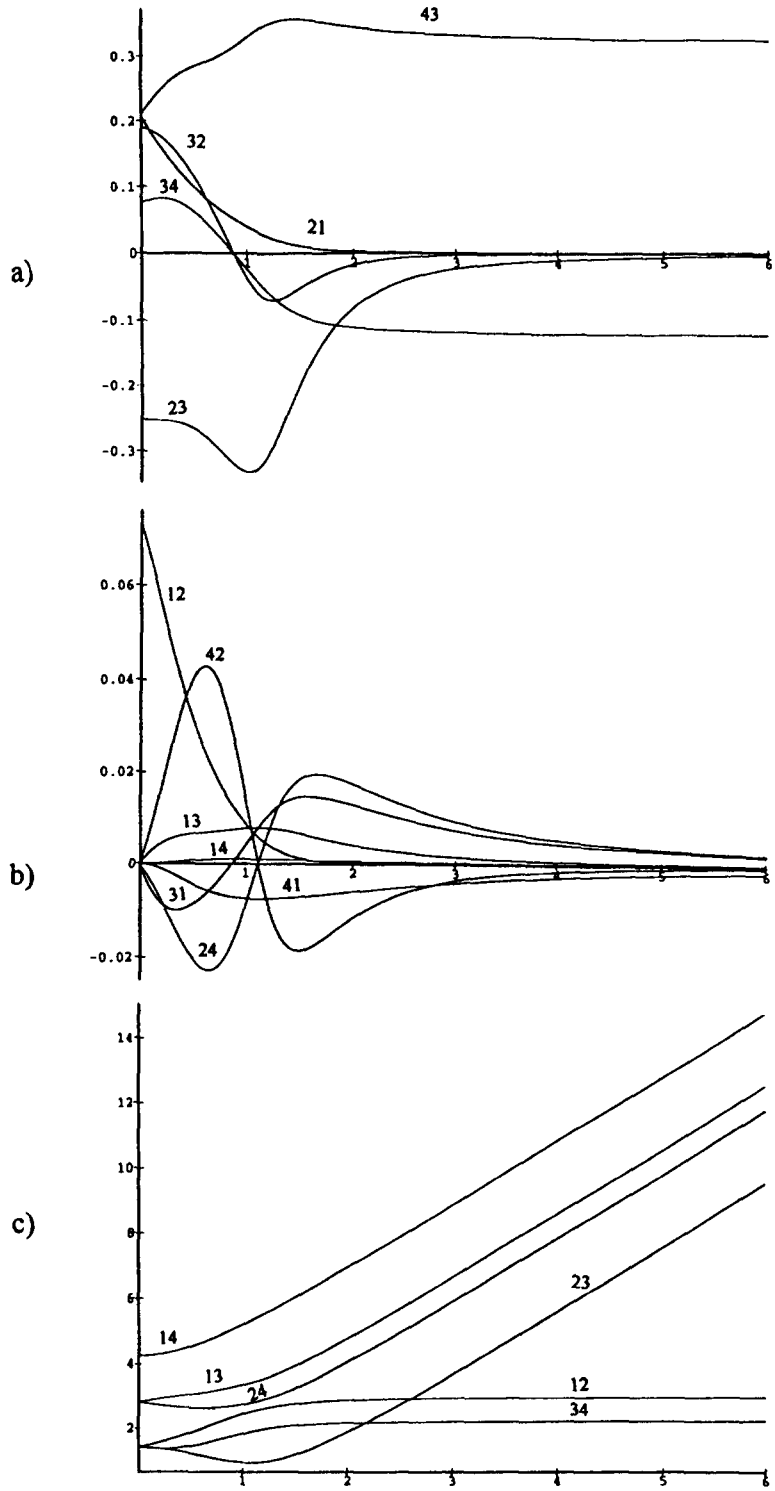

Fig. 1. (a, b) The amplitudes K_{kj}, $K_{kj} = L_{kj}Z_kY_j$, as functions of ω_Q/ω_1 for the case $\Delta\omega = \omega_1$. The numbers relate to the subscripts k and j of K_{kj}. (c) The frequencies ω_{kj}/ω_1 as functions of ω_Q/ω_1 for the case $\Delta\omega = \omega_1$. The numbers relate to the subscripts k and j of ω_{kj}/ω_1.

Table 2
The components $[l, m]$ located at the lth row and mth column of the density matrix $\rho_0(t)$ (Eq. (11)). It is assumed here that each term must be multiplied by L_{kj}, $L_{kj} = 1/2(3X_kX_j + Y_kY_j - Z_kZ_j - 3T_kT_j)$, and summed over k and j. Here $\omega_{kj} = E_k - E_j$

$[11] = 2X_kX_j \cos \omega_{kj}t$, $[22] = 2Y_kY_j \cos \omega_{kj}t$, $[33] = 2Z_kZ_j \cos \omega_{kj}t$, $[44] = 2T_kT_j \cos \omega_{kj}t$
$[21] = Y_kX_j \exp(-i\omega_{kj}t)$, $[31] = Z_kX_j \exp(-i\omega_{kj}t)$, $[32] = Z_kY_j \exp(-i\omega_{kj}t)$,
$[41] = T_kX_j \exp(-i\omega_{kj}t)$, $[42] = T_kY_j \exp(-i\omega_{kj}t)$, $[43] = T_kZ_j \exp(-i\omega_{kj}t)$

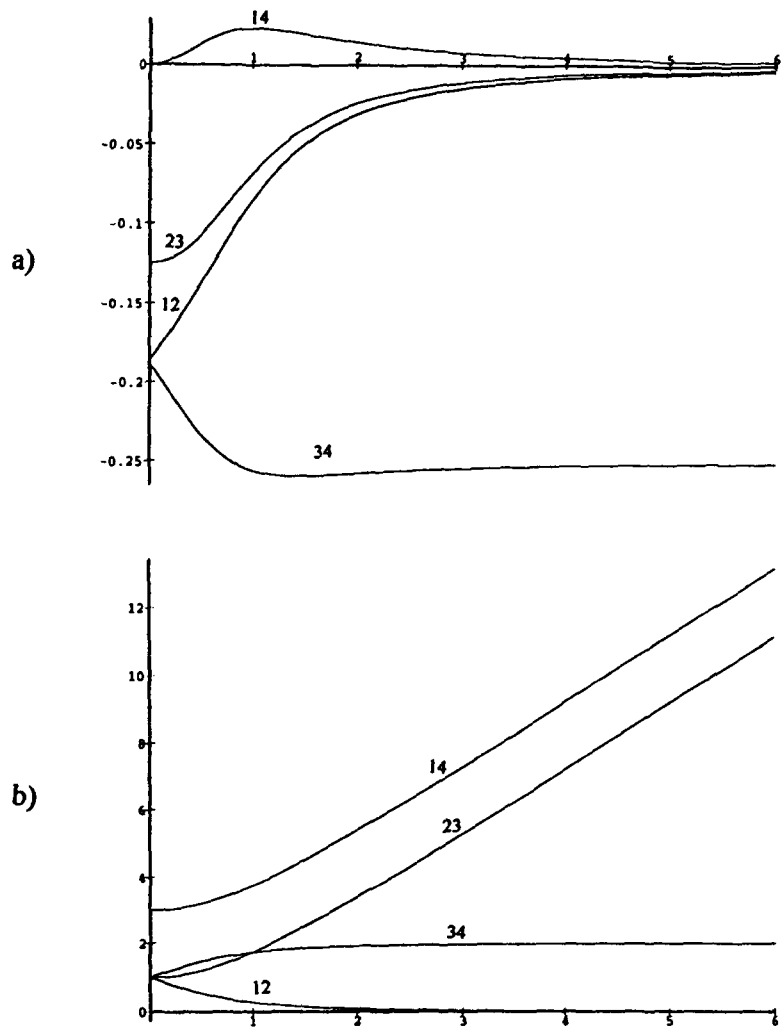

Fig. 2. (a) The amplitudes K_{kj}, $K_{kj} = L_{kj}Z_kY_j$, as functions of ω_Q/ω_1 for the case $\Delta\omega = 0$. The numbers relate to the subscripts k and j of K_{kj}. (b) The frequencies ω_{kj}/ω_1 as functions of ω_Q/ω_1 for the case $\Delta\omega = \omega_1$. The numbers relate to the subscripts k and j of ω_{kj}/ω_1.

The transformation matrix which diagonalizes $H^{(0)}$ and the matrix of eigenvalues are

$$T=\begin{pmatrix} X_1 & X_2 & X_3 & X_4 \\ Y_1 & Y_2 & Y_3 & Y_4 \\ Z_1 & Z_2 & Z_3 & Z_4 \\ T_1 & T_2 & T_3 & T_4 \end{pmatrix},$$

$$E=\begin{pmatrix} E_1 & 0 & 0 & 0 \\ 0 & E_2 & 0 & 0 \\ 0 & 0 & E_3 & 0 \\ 0 & 0 & 0 & E_4 \end{pmatrix}, \qquad (10)$$

respectively, and the equation for the density matrix Eq. (2) becomes

$$\rho_0(t) = T\exp(-\mathrm{i}Et)T^{\mathrm{t}}I_zT\exp(\mathrm{i}Et)T^{\mathrm{t}}. \qquad (11)$$

The calculation of Eq. (11) is performed using MAPLE [7] and the result is given in Table 2. From these one can determine the intensities of the central and satellite lines.

The central line intensities F_x^{32} and F_y^{32} are defined by

$$F^{32} = F_x^{32} + \mathrm{i}F_y^{32} = \rho_0[3,2](t). \qquad (12)$$

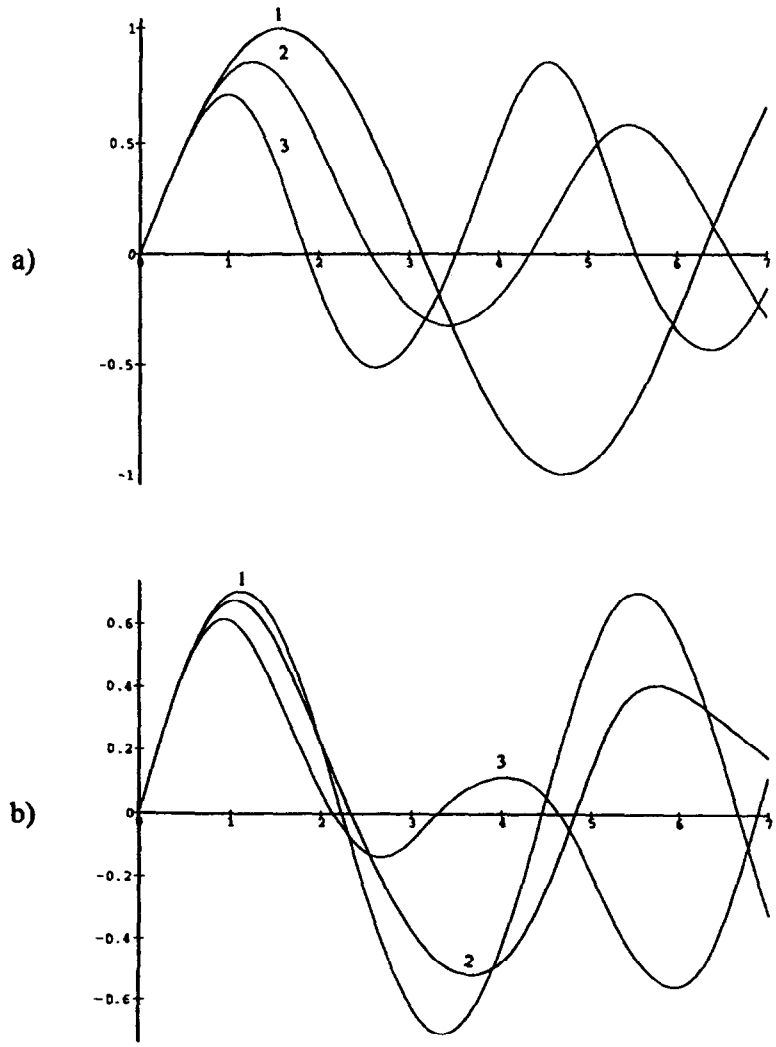

Fig. 3. (a) The line intensity F_y^{32} as a function of the pulse length t in units of $1/\omega_1$ for various ratios of ω_Q/ω_1 for the cases $\Delta\omega = 0$: (1) $\omega_Q/\omega_1 = 0$; (2) $\omega_Q/\omega_1 = 0.5$ and (3) $\omega_Q/\omega_1 = 1$. (b) The line intensity F_y^{32} as a function of the pulse length t for various ratios of ω_Q/ω_1 for the cases $\Delta\omega = \omega_1$: (1) $\omega_Q/\omega_1 = 0$; (2) $\omega_Q/\omega_1 = 0.5$ and (3) $\omega_Q/\omega_1 = 1$.

In general, F_x^{32} is the sum of sixteen terms whereas F_y^{32} is the sum of twelve terms (four of the sixteen terms with $j = k$ are zero), i.e.

$$F_x^{32} = \sum_{k,j=1}^{4} L_{kj} Z_k Y_j \cos \omega_{kj} t, \tag{13}$$

$$F_y^{32} = -\sum_{k,j=1}^{4} L_{kj} Z_k Y_j \sin \omega_{kj} t, \tag{14}$$

where

$$L_{kj} = \tfrac{1}{2}(3X_k X_j + Y_k Y_j - Z_k Z_j - 3T_k T_j) \tag{15}$$

and

$$\omega_{kj} = E_k - E_j. \tag{16}$$

In a similar manner, the intensity of two other possible transitions (satellites) can be found using Table 2. In contrast to the case $\Delta\omega = 0$, these have different offsets of $\Delta\omega + 2\omega_Q$ and $-\Delta\omega + 2\omega_Q$,

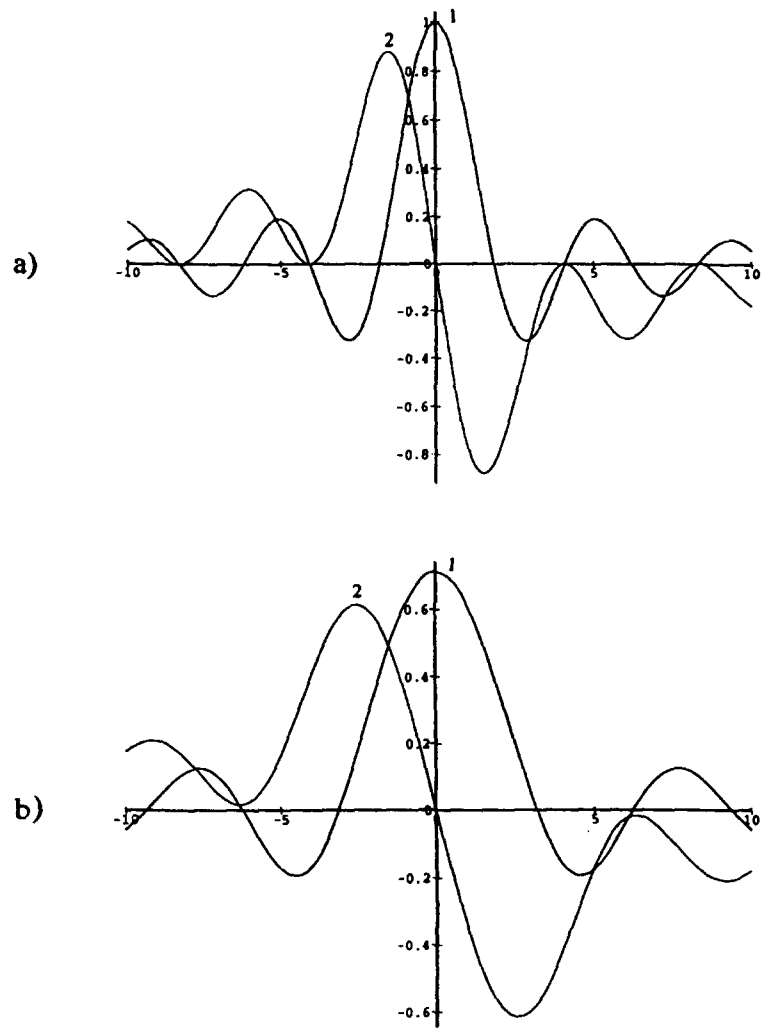

Fig. 4. (a) F_y^{32} (1) and F_x^{32} (2) as functions of $\Delta\omega/\omega_1$ for $\omega_Q = 0$ and $t = 1.5/\omega_1$. (b) F_y^{32} (1) and F_x^{32} (2) as functions of $\Delta\omega/\omega_1$ for $\omega_Q = \omega_1$ and $t = 1/\omega_1$.

respectively, when $\Delta\omega \neq 0$. The line intensities are functions of ω_1, ω_Q and $\Delta\omega$.

Below, we concentrate on the central transition as this is the only one which is usually observed in powders. Eq. (14) can be investigated in the frequency domain. The Fourier transform of these give sets of twelve lines located at ω_{kj}. The amplitudes K_{kj}, $K_{kj} = L_{kj}Z_kY_j$, are shown in Fig. 1a and b as functions of ω_Q/ω_1 for the case $\Delta\omega = \omega_1$. These demonstrate the relative importance of the various contributions from the nutation frequencies. All twelve amplitudes are shown. Fig. 1c depicts six corresponding values of ω_{kj}.

Consider the case $\Delta\omega = 0$. The x component of the line intensity F_x^{32} is reduced to zero for any value of ω_Q whereas F_y^{32} is given by

$$F_y^{32} = 2(L_{12}Z_1Y_2 \sin \omega_{12}t + L_{14}Z_1Y_4 \sin \omega_{14}t + L_{23}Z_2Y_3 \sin \omega_{23}t + L_{34}Z_3Y_4 \sin \omega_{34}t). \quad (17)$$

It should be noted that for this case the matrix of amplitudes is antisymmetric, i.e. $K_{kj} = -K_{jk}$ and $K_{13} = K_{24} \equiv 0$. The latter originates from the fact that the Hamiltonian given in Table 1 can be block diagonalized [8]. The non-zero amplitudes are plotted

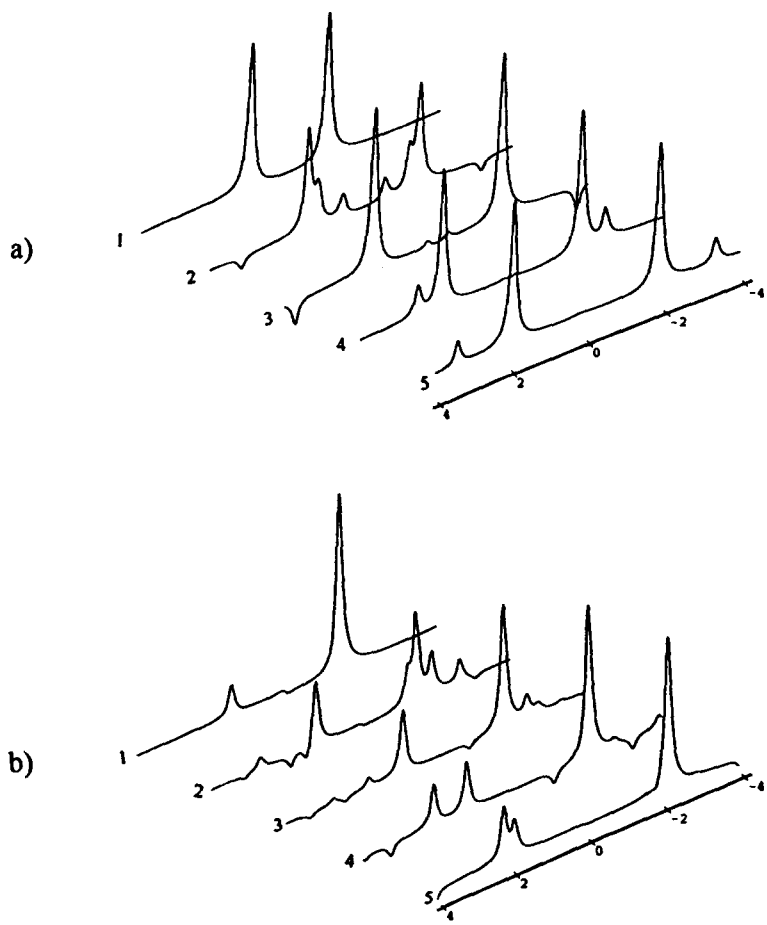

Fig. 5. (a) The imaginary part of $F(\omega)$ (Eq. (18)) as a function of ω/ω_1 for the situation, $T_2 = 10/\omega_1$ and $\Delta\omega = 0$: (1) $\omega_Q/\omega_1 = 0$; (2) $\omega_Q/\omega_1 = 0.5$; (3) $\omega_Q/\omega_1 = 1$; (4) $\omega_Q/\omega_1 = 1.5$ and (5) $\omega_Q/\omega_1 = 2$. (b) The imaginary part of $F(\omega)$ (Eq. (18)) as a function of ω/ω_1 for the situation $T_2 = 10/\omega_1$ and $\Delta\omega = \omega_1$: (1) $\omega_Q/\omega_1 = 0$; (2) $\omega_Q/\omega_1 = 0.5$; (3) $\omega_Q/\omega_1 = 1$; (4) $\omega_Q/\omega_1 = 1.5$ and (5) $\omega_Q/\omega_1 = 2$.

in Fig. 2a as functions of ω_Q/ω_1. The corresponding values ω_{kj} are shown in Fig. 2b. In this case our results are in complete agreement with those of Man [1].

Figs. 3a and b show the line intensity F_y^{32} as a function of the pulse length, t, for various ratios of ω_Q/ω_1 for the cases $\Delta\omega = 0$ and $\Delta\omega = \omega_1$, respectively. It is seen from this figure that, in general, the duration of a $\pi/2$ pulse is a function of ω_1, ω_Q and $\Delta\omega$. We define the duration of a $\pi/2$ pulse as the position at which the response to a $-1+x$ pulse reaches the first maximum when plotted as a function of time. Fig. 4a and b depict the off-resonance profiles of a pulse for the cases $\omega_Q = 0$ and $\omega_Q = \omega_1$. The duration of pulses is chosen to be the duration of a $\pi/2$ pulse. As the value of ω_Q increases, the on-resonance amplitude decreases and the effective width of the curve increases. In the case that $\omega_Q \gg \omega_1$, the pulse becomes selective, and the on-resonance amplitude is half of that in the case when $\omega_Q = 0$. In addition, the width of the curve is twice as broad as in the case $\omega_Q = 0$ because for a selective pulse the rf ω_1 is replaced by the effective frequency $\omega_{1\text{eff}}$, $\omega_{1\text{eff}} = 2\omega_1$ [9].

The FT spectra produced by the system in question can be simulated using Eq. (12). Since satellite transitions are usually lost in the dead time of the receiver, they are not retained. The line broadening is assumed to be Lorentzian, hence the FT of Eq. (12) is

$$F(\omega) = \sum_{k,j=1}^{4} L_{kj} Z_k Y_j \frac{1}{1/T_2 + i(\omega_{kj} - \omega)}. \quad (18)$$

The imaginary part of Eq. (18) is plotted in Fig. 5a and b for the cases $\Delta\omega = 0$ and $\Delta\omega = \omega_1$. In particular, it is seen from Fig. 5 that the spectra exhibit more characteristic powder features in Fig. 5b than in Fig. 5a for higher ω_Q/ω_1 ratios. This is in agreement with Kentgens [5].

Finally, we note that the density matrix $\rho_\phi(t)$ after an rf pulse of an arbitrary phase is [10]

$$\rho_\phi(t)[k, j] = \rho_0(t)[k, j] \exp((k-j)\phi), \quad (19)$$

where the components of the density matrix after the $+x$ pulse, $\rho_0(t)[k, j]$, are given in Table 2. This completes the calculation of the response of spin 3/2 to a pulse of arbitrary amplitude, phase and offset while the first-order quadrupole is active.

3. Conclusions

Here we have presented analytical calculations of the response of a spin 3/2 subject to the first-order quadrupolar interaction and resonance offset while the pulse is on. Our results are in complete agreement with Man's [1] and Kentgen's [5] work in the appropriate limits. Moreover, the inclusion of a resonance offset in the calculation allows for a detailed analysis of a Raman multi-quantum NMR experiment for spin 3/2. It should be noted that practically all 'single' spin interactions can be included into the calculation simply by modifying the constants X, Y and Z in Eq. (7). Currently, most nutation experiments are carried out with magic angle spinning (MAS). It is straightforward to modify our results to include second-order quadrupolar effects. Thus for calculations, such as those in Ref. [11], which use MAS, the CPU time can be dramatically reduced if the second-order interaction is important [12]. Moreover, using computer algebra, it is possible to extend our calculation to at least two pulse sequences with time delay between the pulses.

References

[1] P.P. Man, J. Magn. Reson. 67 (1986) 78; ibid 77 (1988) 148.
[2] P.P. Man, J. Chim. Phys. 89 (1992) 335; P.P. Man, J. Magn. Reson. 100 (1992) 157; P.P. Man, Solid State NMR 1 (1992) 149.
[3] A. Wokaun and R.R. Ernst, J. Chem. Phys. 67 (1977) 1752; S. Vega, J. Chem. Phys. 68 (1978) 5518.
[4] G.J. Bowden, W.D. Hutchison and F. Separovic, J. Magn. Reson. 79 (1988) 413; C.S. Yannoni, R.D. Kendrick and P.K. Wang, Phys. Rev. Letters 58 (1987) 345.
[5] A.P.M. Kentgens, J. Magn. Reson. A 104 (1993) 302.
[6] R.B. Creel, J. Magn. Reson. 52 (1983) 515.
[7] B.W. Char, K.O. Geddes, G.H. Gonnet, B.L. Leong, M.B. Monagen and S.M. Watt, Maple V, Language reference manual, Maple V library reference manual (Springer-Verlag, Berlin, 1993).
[8] A. Samoson and E. Lippmaa, J. Magn. Reson. 79 (1988) 255.
[9] P.P. Man, Appl. Magn. Reson. 4 (1993) 65.
[10] S.Z. Ageev, P.P. Man and B.C. Sanctuary, J. Magn. Reson., in preparation.
[11] S. Ding and C.A. McDowell, J. Magn. Reson. A 112 (1995) 36.
[12] W. Sun, J.T. Stephen, L.D. Potter and Y. Wu, J. Magn. Reson. A 112 (1995) 36.